Electron Tunneling: A Scattering Problem and a Chemical Approach. Interpretation of STM O_2 Image

V. Robert*

Institut de Recherches sur la Catalyse, UPR 5402, 2, avenue Albert Einstein, 69626 Villeurbanne Cedex, France, Ecole normale supérieure de Lyon, Laboratoire de Chimie Théorique, 46, allée d'Italie, 69364 Lyon Cedex 07, France, and Université Claude Bernard de Lyon I, 43, boulevard du 11 novembre 1918, 69622 Villeurbanne Cedex, France

Received: February 9, 1999; In Final Form: May 14, 1999

Within the framework of a scattering model, we investigate the role of electron−electron interactions in the tunneling of electrons between a surface and some adsorbate. The resonant diffusion condition is first derived using a rectangular potential barrier. The participation of exchange−correlation terms is then pointed out by concentrating on a single parameter ξ whose sign determines whether the tunneling s-electron hits resonant diffusion or gets captured in a bound state of the adsorbed molecule. We show that the barrier height and width are affected by the travelling electron which perturbates the molecular energy levels of the adsorbate. For the intriguing problem of O_2, we provide a partial tentative explanation for the experimental STM bump-like image.

1. Introduction

Scanning tunneling microscopy (STM) has been used to extensively study adsorbed molecules on surfaces.[1−3] Some major breakthroughs were made since the very first experiments. However, STM image interpretation remains a challenging issue for experimentalists and theoreticians as well. As a matter of fact, spin-polarized electron tunneling was investigated twenty-five years ago,[4,5] but only recently have model calculations qualitatively showed the importance of spin-resolved density of states.[6,7] Originally, within the framework of tight-binding calculations, the scattering S-matrix method was successfully implemented to describe the elastic scattering process introduced by defect along some one-dimensional periodic chain.[8,9] The electron scattering quantum chemical technique (ESQC) was then extensively developed to get a clearer insight into STM by comparison between experimental and calculated images.[10,11] The transmission probability along the tunneling junction was directly estimated within this approach, and the STM molecular pattern was showed to be strongly dependent on the nature of the adsorbed atom or molecule.[12] The contrast dependence on the atom or molecule binding site was also elucidated.[13] Some qualitative molecular orbital interpretations are now commonly given for images of adsorbates on metallic surfaces.[14] More recently, the influence of the adsorption site as well as geometrical factors on the tunneling current was nicely elucidated on the basis of similar *semiempirical* approaches.[15,16] The success of the ESQC calculations relies on the orbital analysis they provide. Indeed, conclusive interpretations were drawn from molecular orbital descriptions.[14]

Despite its very pictorial form, the ESQC method is probably not appropriate when one deals with adsorbed molecules for which many-electron terms could play a significant role in the current calculation. Indeed, *semiempirical* Hückel-type approaches do not actually take into account electron−electron interactions occurring along the scattering process. The lack of any self-consistent procedure in the energies and orbitals calculations may result in unrelevant image simulations. However, the influence of electronegativity on the calculated topographic profiles of atomic adsorbates was previously considered and conclusive evidence was provided.[12] Small and electronegative atoms, such as oxygen, yield a depression on the STM images. Of major interest is the recent imaging of the O_2 molecule adsorbed on a Pt(111) surface.[17] Unlike the atomic pattern of isolated oxygen atoms, the molecular one reflects a 0.5 Å bump. On the basis of density functional theory calculations using the spin-polarized version of Vienna ab initio simulation program (VASP),[18] it was shown that the bridge site chemisorption of O_2 exhibits a residual spin polarization on the O_2 molecule (0.89 μ_B).[19,20] Using the Mulliken definition, the excess electronic charge on O_2 was estimated at −0.85 with extended Hückel calculations. Since noticeable paramagnetism is maintained upon adsorption, one can assume that the interelectronic contributions may account for such contrast inversion and should be included in a theoretical description. The ESQC approach is certainly not well adapted for these intimate interactions, and a more sophisticated model may be required to reach agreement with experiment.

The growing interest for electron transfer reactions in proteins has given rise to some new theoretical developments.[21] These approaches allow one to study the tunneling current flow between the donor and the acceptor sites of a protein.[22,23] The important point is that they are based on quantum chemistry calculations and therefore can be implemented at any degree of accuracy. In addition, a many-electron formulation was proposed to calculate the tunneling matrix element, a key parameter in electron transfer reactions.[24,25] Following this trend of quantitative approaches, a description of the electron transfer process between two reservoirs of states was nicely depicted elsewhere.[26] A scattering formalism was used to express the conductance arising from the connection of two noninteracting reservoirs through some one-dimensional wire. Several inter-

* Corresponding author fax, (33) (0)4 72 44 53 99; e-mail: vrobert@ens-lyon.fr.

10.1021/jp990488u CCC: $18.00
Published on Web 08/05/1999

pretations were drawn regarding the quantum nature of the wire in the tunneling process.[27]

The many-electron Stuchebrukhov's formulation makes it possible to include the crucial interelectronic interactions giving rise to polarization effects.[21−25] Similarly, the Green's function formalism pointed out the importance of the electron−electron interactions.[26,27] Even though quantitative comparisons with experiment might result, ab initio descriptions include sophisticated details that one could bypass when investigating complicated issues. Quantitative approaches do not provide a straight chemical picture of the factors which control the electron transfer rate. On the basis of a scattering approach, we were concerned with the featuring interactions of the tunneling electron with the other electrons. Our purpose was to look for the electronic parameters which may qualitatively control the current intensity along the tunneling process. The simplest picture is given by a potential step the electron must go through. Thus, we investigated the consequences of changes in the potential the scattered electron experiences when tunneling occurs. A similar method, namely the "coupled angular modes" method (CAM), was developed to study the position and width of negative ion C^- in front of a surface.[28,29] However, our goal was to qualitatively go beyond the effective range approximation which reduces the scattering problem to some outer region where the electron radial wave function is calculated. The issue was also somewhat different since we were primarily interested in estimating the electron diffusion from the bulk through some adsorbed molecule. We believe that if one can trace the modulation of the scattering cross-section as a function of electron−electron interactions, a clearer and more intuitive feel for what is observed in STM experiments might result. In the next sections, we provide the details of our qualitative model we have used to assess the role of these interelectronic contributions to the tunneling current. We then apply this model to trace the variations in the tunneling rate through adsorbed dioxygen on a platinum (111) surface.

2. Description of the Model

Since our goal is to give a new qualitative analysis of the scattering process, one should recall the fundamental description of electron tunneling. Let us assume that an electron is shot from a metallic system on some adsorbed molecule at a surface. The electron clearly experiences interactions with the molecule and, as a particularly interesting issue, with all the electrons through Coulomb and exchange−correlation contributions. A schematical picture of the phenomenon is given in Figure 1 where (R), (AM), and (V) stand for the reservoir, the adsorbed molecule, and the vacuum, respectively. Since these are the three regions of space the electron travels through, the perturbation associated with the presence of the scanning tunneling microscope tip is not taken into account in our model. The important role of the tip in the tunneling current calculation is not explicitly taken into account and left for future investigations. We are exclusively concerned with the tunneling phenomenon originated by the surface−adsorbate system.

In the reservoir, the electron-state is well described within a nearly free particle approach.[30] The wave function takes the usual Bloch function form

$$\psi_{\vec{\theta}}(\vec{r}) = u_{\vec{\theta}}(\vec{r})\cdot e^{-i\vec{\theta}\cdot\vec{r}} \qquad (1)$$

where $u_{\vec{\theta}}$ has the periodicity L of the lattice. For the sake of simplicity, the propagation is assumed to occur along a single direction, namely z and $z \leq 0$ in the reservoir (see Figure 1).

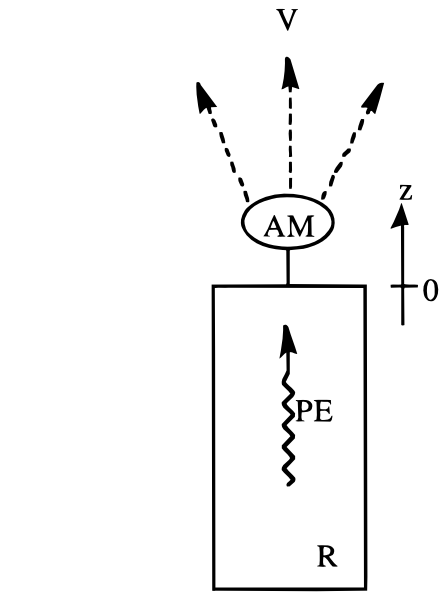

Figure 1. Schematical representation of the tunneling process. (R), (PE), (AM), and (V) stand for reservoir, propagating electron, adsorbed molecule, and vacuum, respectively.

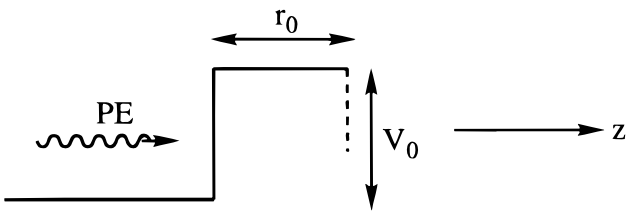

Figure 2. Representation of the rectangular step the propagating electron must step over when tunneling occurs.

Therefore, eq 1 may be written as

$$\psi_\theta(z) = u_\theta(z)\cdot e^{-i\theta\cdot z} \qquad (2)$$

where θ stands for the wave vector component along z. Thus, the description of the electron in the reservoir (R) is a one-dimensional propagating wave schematically represented in Figure 1. It should be emphasized at this point that as long as the position z is not significantly varied, i.e., $|\Delta z| \ll L$, ψ is reduced to the travelling plane-wave of a free electron at the Fermi level with energy $\epsilon_F = (\hbar^2\theta^2)/2m$. In the following discussion, ϵ_F is chosen as a reference energy. Even though a natural description of the electron would obviously be given by a wave packet of group velocity $\hbar\theta/m$, it is well admitted that a satisfactory approach relies on the stationary states calculations. This is the one we consider in this paper.

Here we suppose that the long-range potential of the adsorbed molecule does not significantly perturbate this description in the reservoir. However, when reaching the surface $z = 0$, the propagating electron experiences the influence of the adsorbate. One may model this interaction by including a rectangular potential barrier that the electron must step over in the scattering event. Thus, we assume that the potential can be characterized by its height $V_0 = (\hbar^2 k_0^2)2m$ and its width r_0 (Figure 2). The former takes into account the details of the adsorbate electronic levels, whereas the latter is related to the spatial range of the potential corresponding to the electronic density of the adsorbate. In a very intuitive way, V_0 can be seen as the energy gap between the Fermi level and some effective molecular orbital energy of the adsorbate. Using an elementary picture, this orbital can be approximated by a Slater-type orbital (STO). Since

contracted orbitals originate strong electron−electron repulsion, the more diffuse the orbital, the smaller the barrier height. In addition, diffuse orbitals strongly overlap and facilitate the transfer of the tunneling electron. Thus, r_0 might be directly connected to the extension coefficient of the effective STO. When the travelling electron reaches the scattering species, these two parameters are modulated by the interelectronic exchange and correlation interactions. In the presence of the scanning tip, the tunnel gap between the tip and the adsorbate is also reduced by more diffuse orbitals (i.e., smaller barrier width). In the near future, we intend to improve the model by including a second barrier that would describe the tunneling gap between the adsorbed molecule and the tip.

Within this picture, the issues that have to be addressed are the following: (1) How much can the barrier characteristics V_0 and r_0 be controlled by the electron−electron interactions in the region of space $r > r_0$? (2) Does the symmetry of the valence orbitals influence this rate? (3) Does the spin part of the wave function play a role in the current control?

To answer these questions, we first reworked the scattering problem giving rise to either a bound state or a resonant diffusion. It should be pointed out that as soon as the propagating electron undergoes resonant diffusion, one should expect an increase in the tunneling current.

3. Bound State and Resonant Diffusion at Low Energy

Let us consider an adsorbed species on a metallic surface with local spherical symmetry. The description of the electron in terms of a plane wave near the surface can be expanded into spherical harmonics as

$$e^{i\theta z} = \sum_l i^l \sqrt{4\pi(2l+1)} j_l(\theta r) Y_{l,0}(\Theta)$$

where j_l is the spherical Bessel function. The CAM method states that the electron−metal interaction potential mixes the different angular scattering modes of the molecule.[28] However, it was demonstrated that the long-range potentials arising from centrifugal and polarization effects are separated as long as the electron-scattering adsorbate distance r satisfies $r \approx r_0$. Besides, a diabatic description of the electron−metal interaction is well adapted since the angular momentum l can be considered as a good quantum number.[28] Such approximation relies on the assumption that the spherical symmetry in the vicinity of the atom is not significantly altered. Therefore, we assume that the Schrödinger equation can be solved for each value of l and the travelling electron wave function reduces to $\psi_{travel} = \mu(r)/r \cdot Y_{l,0}$.

Within the framework of these approximations, the time-independent Schrödinger equation for the radial part is in atomic units

$$\left[-\frac{d^2}{dr^2} + \frac{l(l+1)}{r^2} + V(r)\right]u = \rho^2 u \tag{3}$$

Following our model, in the reservoir equation (eq 3) takes the usual form

$$\left[-\frac{d^2}{dr^2} + \frac{l(l+1)}{r^2} - k_0^2\right]u = \rho^2 u \text{ for } r < r_0 \tag{4a}$$

and

$$\left[-\frac{d^2}{dr^2} + \frac{l(l+1)}{r^2}\right]u = \rho^2 u \text{ for } r > r_0 \tag{4b}$$

Let us focus on the scattering of s-states (i.e., $l = 0$) as they are known to contribute most to the total current. The procedure used to solve these equations was developed elsewhere and gives rise to two sets of solutions depending on the energy.[31] If negative, then $\rho = ik$, $k < k_0$, and the continuity of the wave function and its first derivative may be written as

$$tg(Kr_0) = -\frac{K}{k} \text{ with } K = \sqrt{k_0^2 - k^2} \tag{5}$$

If $Kr_0 < \pi/2$, eq 5 does not hold any solution and no bound s-state is found.

On the other hand, if the energy is positive, $\rho = k$ and the continuity conditions reduce to

$$B^2 = \frac{k^2}{k^2 + k_0^2 \cos^2(K' r_0)} \text{ and } K' = \sqrt{k_0^2 - k^2} \tag{6}$$

where B is the amplitude of the sinusoidal solution of (4a) $u(r) = B\sin(K'r)$, whereas a solution for (4b) is written in the usual form $u(r) = \sin(kr + \delta_0)$. The resonance condition emerging from eq 6 is

$$K' r_0 = (2n+1)\frac{\pi}{2} \tag{7}$$

Within the low-energy limit, $|kr_0| \ll 1$, it is easily shown that

$$k_0 r_0 \approx \delta_0 = (2n+1)\frac{\pi}{2} \tag{8}$$

This well-known expression is consistent with the calculation of the scattering cross-section.[31] A maximum is reached for an s-state of a given energy as soon as condition (8) is satisfied.

A more interesting point arising from eq 8 is that the resonance condition relies on the characteristics of the barrier. Indeed, the adsorbed molecule generates a potential whose height and width directly control the flow of electron. However, along the scattering event these parameters are modified as a result of electron−electron interactions. Thus, we introduced one additional parameter ξ which accounts for the modulations of k_0 and r_0 ($|\xi| \ll 1$). In the vicinity of resonance, eq 8 may then be written as

$$k_0 r_0 = (2n+1)\frac{\pi}{2} + \xi \tag{9}$$

It is easily established that as the sign of ξ changes, the system undergoes a transition from a bound state to a resonant one. Indeed, if $\xi > 0$ then the continuity condition (eq 5) becomes

$$k^2 \approx \xi^2 k_0^2 \tag{10}$$

whereas if $\xi < 0$, the resonance condition (eq 7) gives

$$k^2 \approx \frac{-2\xi k_0}{r_0} \tag{11}$$

The low-energy states associated with the wave vectors eqs 10 and 11 correspond to a bound state and a resonant diffusion, respectively. In other words, as soon as eq 11 is satisfied, i.e., $\xi < 0$, one should observe an increase of the tunneling current. As the travelling electron reaches the vicinity of the adsorbed

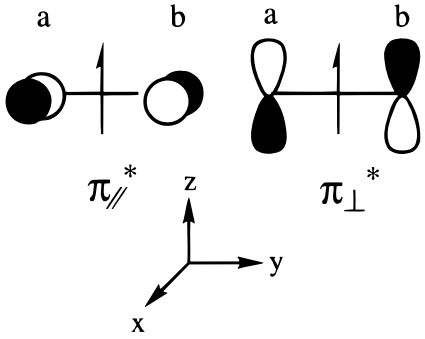

Figure 3. Highest occupied molecular orbitals of O_2. $\pi_{||}^*$ and $\pi_\perp^*$ remain quasi-degenerate with adsorption.

molecule, the potential properties it experiences are changed and electron−electron interactions could play the role of a dimmer switch. The assumption $|\xi| \ll 1$ is consistent with the perturbating contribution of interelectronic terms to the core Hamiltonian.

In the next section we investigate the magnitude of these interactions resulting in the modification of the potential barrier properties. Our purpose is to trace the changes in the ξ parameter in the vicinity of any resonant diffusion state (equations 8 and 9). Special attention is given to the comparison between atomic oxygen and molecular dioxygen adsorptions.

4. Electron−Electron Interactions: A Tunneling Control in O_2

Let us first focus on a different issue to understand the orbital changes accompanying bond formation. A very nice picture was given by J. K. Burdett.[32] The author showed that, owing to the virial theorem, the magnitude of the potential energy determines the stablilization energy of H_2^+. The origin lies in the contraction of the 1s orbitals with respect to the free atoms. In extended Hückel theory, this phenomenon is reflected by the value 1.3 of the hydrogen 1s expansion coefficient, whereas it is 1.0 for the isolated atom.[33] This is a general trend that accounts for the reduction of the potential energy when any atom is involved in chemical bonding. The valence radius shell contraction is explicitly taken into account when the adsorption mechanism is studied. However, if one compares the valence orbitals of adsorbed dioxygen O_2 and adsorbed oxygen O, the main difference lies in the composition of the dioxygen highest π^* occupied molecular orbitals $\pi_{||}^*$ and $\pi_\perp^*$ (HOMOs in Figure 3). The orbitals are labeled according to their symmetry with respect to the surface. From the LCAO method, it is well established that if y stands for the molecule axis, $\pi_{||}^* = 1/[2(1 - S)]^{1/2}(p_x^a - p_x^b)$ and $\pi_\perp^* = 1/[2(1 - S)]^{1/2}(p_z^a - p_z^b)$ where S is the overlap integral between atomic orbitals $\{p_\alpha^\sigma\}_{\sigma=a,b}^{\alpha=x,z}$ localized on atom a and b (see Figure 3). Because of the antibonding character of $\pi_{||}^*$ and $\pi_\perp^*$, the depletion of electron density between the oxygen nuclei results in more diffuse orbitals than that of the isolated atoms. Let us now consider the formation of O_2 from O atoms on the surface. As just pointed out, the range r_0 of the effective potential resulting from the antibonding π^*-system decreases. In the vicinity of resonant diffusion (see eq 9), the STO contraction results in a negative ξ value. The tunneling current increases (eq 11) and a noticeable corrugation between O and O_2 should be observed. Recent experimental studies showed that O_2 on Pt(111) looks like a bump[17] ("large" current), whereas it was previously demonstrated[12] that O on Pt(111) displays a depression ("small" current). Even though this very naive model does not take into account the presence of any tip, agreement with experiment lies in the more diffuse character of the O_2 valence orbital relative to that of the free oxygen atoms. We should point out that the interpretation based on a negative ξ value resulting from orbital extension is consistent with the exponential decay of the tunneling current with the barrier width r_0. As far as the relative barrier heights of O and O_2 are concerned, no conclusion can be brought about since the electronic levels of the two systems are very different from one another. The accurate calculations of the energy level changes are out of the scope of this paper.

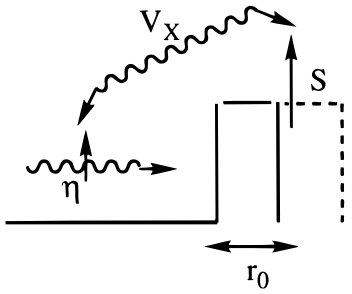

Figure 4. Strong exchange interaction V_X between the propagating electron and the O_2 high spin state. The barrier height is reduced.

The interelectronic interactions may then be included in our model to give a more detailed picture of the scattering potential variations. The valence molecular orbitals of O_2 are shown in Figure 3.

We here focus on the valence orbitals $\pi_{||}^*$ and $\pi_\perp^*$ which are both singly occupied and bear spin states $|S_1, M_{S_1}\rangle = |1/2,1/2\rangle$ and $|S_2, M_{S_2}\rangle = |1/2,1/2\rangle$. The splitting of these orbitals with adsorption on a bridge site is small enough so that, as a first approximation, the molecule spin state might not be altered. Ab initio calculations were performed to support this statement. Indeed, the density of states projected on $\pi_{||}^*$ and $\pi_\perp^*$ orbitals are maximum at −0.08 eV and 0.40 eV with a reference energy at the Fermi level.[20] Let us first assume that the spin state $|S,M_s\rangle$ of the O_2 molecule is triplet as in the gas phase, i.e., $S = S_1 + S_2 = 1$. The travelling electron bears a spin η, and we assume that the spin state is $|\eta, M_\eta\rangle = |1/2, 1/2\rangle$ (Figure 4). Since the total spin S_T must satisfy $|S - 1/2| \le S_T \le |S + 1/2|$, $S_T = 1/2$ and $S_T = 3/2$ are the two possible values. The latter exhibits strong exchange interaction V_X, as $M_{S_1} = M_{S_2} = M_\eta = 1/2$ is consistent with $S_T = 3/2$ (see Figure 4). The Pauli principle excludes the propagating electron from being at the same place at the same time of any of the two electrons of paramagnetic O_2. Therefore, the strong Coulomb repulsion results in more diffuse $\pi_{||}^*$ and $\pi_\perp^*$ orbitals. As shown in Figure 4, r_0 decreases and a negative ξ value results. As mentioned before, the tunneling current is enhanced. More recently, the spin polarization[20] ($\mu = 0.89\ \mu_B$) as well as a negative charge (−0.85) on an adsorbed O_2 molecule have been calculated. The former value suggests that the spin state of O_2 might be better described as a doublet $S = 1/2$, for then the orbital paramagnetism being quenched, $\mu = [S(S + 1)]^{1/2}\mu_B \approx 0.86\ \mu_B$. However, the conclusions previously derived for the triplet spin state remain valid. Even though some part of the electronic density is reflected and does not contribute to the current, the transmission coefficient is increased as compared to a bound state with $\xi > 0$. The exchange contribution to the scattering cross-section evaluation was pointed out elsewhere with a slightly different point of view.[34]

Another mechanism influencing the tunneling current is supported by the perturbation of O_2 levels $\pi_{||}^*$ and $\pi_\perp^*$ by ψ_{travel}. Let us qualitatively derive the energy level changes shown in

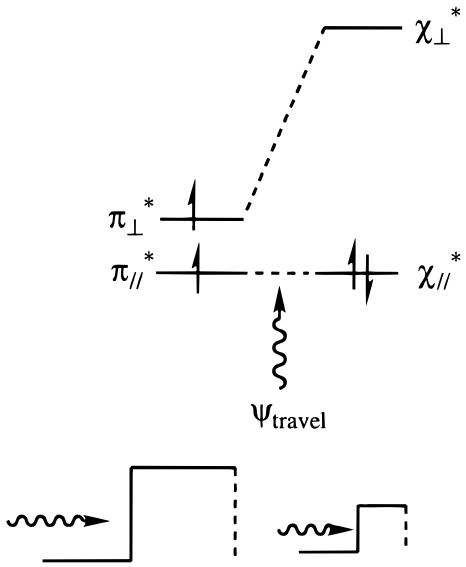

Figure 5. Interactions between ψ_{travel} and $\pi_{||}^*$ and $\pi_{\perp}^*$. The spin state transition results in a smaller barrier height and a smaller barrier width schematically depicted.

Figure 5. Second-order perturbation theory states that the greater the overlap and the smaller the energy difference, the larger the interaction. ψ_{travel} is mainly polarized along the *z*-axis, whereas $\pi_{||}^*$ lies in the *xy*-plane. Therefore, upon interaction the latter does not significantly change in energy. Conversely, even if slightly higher in energy than $\pi_{||}^*$, $\pi_{\perp}^*$ is more destabilized owing to axial overlap along the *z*-axis. Our main assumption relies in the s-character of the scattering electron. We should stress that the interaction $\psi_{travel} - \pi_{\perp}^*$ is different from zero as long as the electron travels off the nodal plane of $\pi_{\perp}^*$. Previous calculations showed that this particular configuration is likely to occur since the O_2 bridges two platinum surface atoms.[19,20] The O_2 orbitals resulting from the interaction are labeled $\chi_{||}^*$ and $\chi_{\perp}^*$, respectively (see Figure 5). In the following discussion, we assume that a three-electron interaction occurs and that the oxygen molecule spin state is either singlet or triplet.

We now turn to investigate the singlet−triplet energy difference E_{S-T} in O_2 in the presence and in the absence of the interacting travelling electron. The triplet energy is easily estimated, whereas the singlet energy determination requires some development.[35,36] We briefly recall the theoretical development given in ref 35 to estimate the singlet−triplet energy difference. For the sake of simplicity, we define ψ_1 and ψ_2, with $\psi_1 = \pi_{||}^*$ or $\chi_{||}^*$ and $\psi_2 = \pi_{\perp}^*$ or $\chi_{\perp}^*$. The lowest singlet state is a mixture of $|\psi_1\bar{\psi}_1|$ and $|\psi_2\bar{\psi}_2|$ which is determined by solving the secular equation

$$\begin{vmatrix} 2H_1^c + J_{11} - E & K_{12} \\ K_{12} & 2H_2^c + J_{22} - E \end{vmatrix} = 0 \qquad (12)$$

where H^c represents the core operator consisting of the kinetic energy, nuclear attraction, and all other electron repulsion. $J_{ij} = (\psi_i\psi_j|\psi_i\psi_j)$, $K_{ij} = (\psi_i\psi_j|\psi_j\psi_i)$ are the Coulomb and exchange terms, respectively. The respective energies are as follows:

$$E_T = H_1^c + H_2^c + J_{12} - K_{12}$$

$$E_S = H_1^c + H_2^c + 1/2(J_{11} + J_{22}) - 1/2\{[2(H_1^c - H_2^c) + J_{11} - J_{22}]^2 - 4K_{12}^2\}^{1/2} \qquad (13)$$

Thus, the singlet−triplet splitting E_{S-T} takes the following form:

$$E_{S-T} = 1/2(J_{11} + J_{22}) - 1/2\{[2(H_1^c - H_2^c) + J_{11} - J_{22}]^2 - 4K_{12}^2\}^{1/2} - (J_{12} - K_{12}) \qquad (14)$$

It is more useful to define the usual orthogonal magnetic orbitals (OMO)[36] ψ_a and ψ_b as follows:

$$\psi_a = \frac{1}{\sqrt{2}}(\psi_1 + \psi_2) \qquad \psi_b = \frac{1}{\sqrt{2}}(\psi_1 - \psi_2) \qquad (15)$$

Equation 14 then becomes

$$E_{S-T} = 2K_{ab} - \frac{(\epsilon_1 - \epsilon_2)^2}{J_{aa} - J_{ab}} \qquad (16)$$

where ϵ_1 and ϵ_2 are the energies defined by the Hartree−Fock operator for the triplet state orbitals, i.e., $\epsilon_i = H_i^c + J_{12} - K_{12}$. In the absence of the travelling electron ($\psi_1 = \pi_{||}^*$, $\psi_2 = \pi_{\perp}^*$), $J_{aa} > J_{ab}$, $\epsilon_1 \approx \epsilon_2$ and the triplet is favored over the singlet. However, when the electron reaches the surface, the splitting is increased, $\epsilon_2^* \gg \epsilon_1^*$ (see Figure 5) since ψ_{travel} strongly interacts with $\pi_{\perp}^*$ and a singlet ground state for O_2 results. Hence, the O_2 molecule is likely to undergo a triplet−singlet transition, the singlet ground-state main contribution being $|\chi_{||}^*\bar{\chi}_{||}^*|$. Thus, the paired electrons being in the same orbital are allowed to come closer to one another, resulting in a stronger repulsion. The effective valence shell radius must automatically expand, and r_0 contract, for the strong correlation effects thereby to be taken into account. Besides, the barrier height is lowered by approximately $|E_{S-T}|$ (see Figure 5) and k_0 decreases. As previously mentioned, a negative ξ value results, the scattering process hits resonance, and the tunneling current is increased.

The mechanism we describe here takes into account the influence of the propagating electron on the electronic properties of the scattering center. The two spin states we considered lead to a negative ξ parameter, a reflection of a high tunneling intensity. On the basis of our scattering model, qualitative agreement is reached with experiment regarding the bump-shape of O_2 image.

5. Conclusion

Using a simple s-scattering approach, we tried to emphasize the control of the tunneling rate through the value of a single key parameter, namely ξ. As a matter of fact, ξ accounts for any change in the barrier characteristics r_0 and k_0. In the vicinity of resonance diffusion, a negative sign corresponds to a greater current. We first showed that the electron−electron interactions might be responsible for the r_0 and k_0 variations. A reduction of any of these two parameters results in a negative ξ value. For the intriguing problem of O_2 STM images, we were then able to identify the mechanisms involving the adsorbed molecule and the travelling electron represented in a rough approximation as a plane wave. A more accurate description of the propagating electron would be given by a wave packet, but such an approach is left for future publication. Despite its qualitative framework, our model made it possible to give some new insights into the way the scattered electron perturbates the energy levels of O_2 as it gets close to the surface. It provides an intuitive feel for the modulations of k_0, a measure of the energy difference between the Fermi level and the quasi-degenerate $\pi_{||}^*$ and $\pi_{\perp}^*$ orbitals, as well as for the changes in the potential range

amplitude r_0 associated with the π^* network. We showed that the exclusion principle and the triplet−singlet transition in O_2 reduce the barrier parameters and that the tunneling current increases. This approach may easily be extended to any other similar problem where the adsorbed species is partly paramagnetic. Besides, the influence of the metal magnetization might also be included in our approach in relation with the spin-polarized STM technique. We finally intend to explicitly take into account the role of temperature, particularly important in the filling of the spin states. Within a temperature-dependent model, we should be able to investigate the tunneling current intensity as a function of temperature for systems with greater numbers of spin multiplets.

Acknowledgment. The author thanks Dr. Serguei Borshch and Dr. John Brennan for having carefully read the manuscript. Dr. M-L Bocquet was extremely enlightening on the STM issue.

References and Notes

(1) Hallmark, V. M.; Chiang, S.; Meinhardt, K.-P.; Hafner, K. *Phys. Rev. Lett.* **1993**, *70*, 3740.
(2) Hallmark, V. M.; Chiang, S. *Surf. Sci.* **1995**, *329*, 255.
(3) Biscarini, F.; Bustamante, C.; Kenkre, V. M. *Phys. Rev. B* **1995**, *51*, 11089.
(4) Tedrow, P. M.; Meservey, R. *Phys. Rev. Lett.* **1971**, *26*, 192.
(5) Tedrow, P. M.; Meservey, R. *Phys. Rev. B* **1973**, *7*, 318.
(6) Bürgler, D.; Tarrach, G. *Ultramicroscopy* **1992**, *42*, 194.
(7) Petrov, E. G.; Tolokh, I. S. *J. Chem. Phys.* **1998**, *108*, 4386.
(8) Landauer, R. *Philos. Mag.* **1970**, *21*, 863.
(9) Anderson, P. W.; Thouless, D. J.; Abrahams, E.; Fisher, D. S. *Phys. Rev. B* **1980**, *22*, 3519.
(10) Sautet, P.; Joachim, C. *Phys. Rev. B* **1988**, *38*, 12238.
(11) Sautet, P.; Joachim, C. *Chem. Phys. Lett.* **1991**, *185*, 23.
(12) Sautet, P. *Surf. Sci.* **1997**, *374*, 406.
(13) Sautet, P.; Bocquet, M.-L *Surf. Sci.* **1994**, *304*, L445.
(14) Sautet, P.; Bocquet, M.-L *Phys. Rev. B* **1996**, *53*, 4910.
(15) Bocquet, M.-L.; Sautet, P. *Surf. Sci.* **1996**, *360*, 128.
(16) Bocquet, M.-L.; Sautet, P. *Surf. Sci.* **1998**, *415*, 148.
(17) Stipe, B. C.; Rezaci, M. A.; Ho, W.; Gao, S.; Pessron, M.; Lundqvist, B. I. *Phys. Rev. Lett.* **1997**, *78*, 4410.
(18) (a) Kresse, G.; Hafner, J. *Phys. Rev. B* **1994**, *49*, 14251. (b) Furthmüller, J.; Kresse, G.; Hafner, J. *Phys. Rev. B* **1994**, *50*, 15606.
(19) Eichler, A.; Hafner, J. *Phys. Rev. Lett.* **1997**, *79*, 4481.
(20) Bocquet, M.-L, Cerdá, J.; Sautet, P. *Phys. Rev. B* **1999**, in press.
(21) Stuchebrukhov, A. A. *J. Chem. Phys.* **1996**, *104*, 8424.
(22) Stuchebrukhov, A. A. *J. Chem. Phys.* **1996**, *105*, 10819.
(23) Stuchebrukhov, A. A. *J. Chem. Phys.* **1997**, *107*, 6495.
(24) Stuchebrukhov, A. A. *J. Chem. Phys.* **1998**, *108*, 8499.
(25) Stuchebrukhov, A. A. *J. Chem. Phys.* **1998**, *108*, 8510.
(26) Mujica, V.; Kemp, M.; Ratner, M. A. *J. Chem. Phys.* **1994**, *101*, 6849.
(27) Mujica, V.; Kemp, M.; Ratner, M. A. *J. Chem. Phys.* **1994**, *101*, 6856.
(28) Teillet-Billy, D.; Gauyacq, J. P. *Surf. Sci.* **1990**, *239*, 343.
(29) Teillet-Billy, D.; Gauyacq, J. P.; Nordlander, P. *Surf. Sci. Lett.* **1997**, *371*, L 235.
(30) Kittel, C. *Introduction to Solid State Physics*; Wiley: New York, 1986.
(31) Cohen-Tannoudji, C.; Diu, B.; Laloë, F. *Mécanique Quantique*, Hermann: Paris, 1992.
(32) Burdett, J. K. *Chemical Bonds: A Dialogue*; Wiley: Chischester, 1997.
(33) Hoffmann, R. *J. Chem. Phys.* **1963**, *39*, 1397.
(34) Landau, L.; Lifchitz, E. *Mécanique Quantique*; Mir: Moscou, 1975.
(35) Hay, P. J.; Thibeault, J. C.; Hoffmann, R. *J. Am. Chem. Soc.* **1975**, *97*, 4884.
(36) De Loth, P.; Daudey, J.-P.; Malrieu, J.-P. *J. Am. Chem. Soc.* **1981**, *103*, 4007.